and Dr. Y. S. Chen, Dr. T. A. Tombrello, and Dr. R. W. Kavanagh for sending us their ^{9}Li results prior to publication. One of us (C.L.C.) acknowledges financial support from the Institut de Recherches Nucléaires. He especially wishes to express his thanks to Dr. S. Gorodetsky and Dr. P. Chevallier for making his stay at Strasbourg a profitable and enjoyable one.

---

*Present address: Kansas State University, Manhattan, Kansas.

†National Science Foundation Postdoctoral Fellow, 1968–1969.

[1]E. G. Adelberger, C. L. Cocke, C. N. Davids, and A. B. McDonald, Phys. Rev. Letters 22, 352 (1969).

[2]A. B. McDonald, E. G. Adelberger, H. B. Mak, D. Ashery, A. P. Shukla, C. L. Cocke, and C. N. Davids, Phys. Letters 31B, 119 (1970).

[3]G. M. Griffiths, Nucl. Phys. 65, 647 (1965).

[4]F. S. Dietrich, M. Suffert, A. V. Nero, and S. S. Hanna, Phys. Rev. 168, 1169 (1968).

[5]C. L. Cocke, J. C. Adloff, and P. Chevallier, Phys. Rev. 176, 1120 (1968).

[6]G. A. Peterson, Phys. Letters 25B, 549 (1967).

[7]G. Wittwer, H. G. Clerc, and G. A. Beer, Phys. Letters 30B, 634 (1969).

[8]E. K. Warburton and J. Weneser, in *Isospin in Nuclear Physics*, edited by D. H. Wilkinson (North-Holland Publishing Company, Amsterdam, The Netherlands, 1969), p. 173.

[9]G. M. Temmer, B. Teitelmann, R. Van Bree, and H. Ogato, J. Phys. Soc. Japan Suppl. 24, 299 (1968).

[10]M. J. Le Vine and P. D. Parker, Phys. Rev. 186, 1021 (1969).

[11]K. A. Snower, E. G. Adelberger, and F. Riess, Bull. Am. Phys. Soc. 13, 1662 (1968).

[12]A. Amit and A. Katz, Nucl. Phys. 58, 388 (1964).

[13]S. Cohen and D. Kurath, Nucl. Phys. 73, 1 (1965).

[14]F. C. Barker, Nucl. Phys. 83, 418 (1966).

[15]B. E. F. Macefield, B. Wakefield, and D. H. Wilkinson, Nucl. Phys. A131, 136 (1969).

[16]Y. S. Chen, T. A. Tombrello, and R. W. Kavanagh, Nucl. Phys. A146, 136 (1970).

[17]T. Lauritsen and F. Ajzenberg-Selove, Nucl. Phys. 78, 1 (1966).

[18]H. G. Clerc, K. J. Wetzel, and E. Spamer, Phys. Letters 20, 667 (1966).

[19]B. Lynch, G. M. Griffiths, and T. Lauritsen, Nucl. Phys. 65, 641 (1965).

[20]P. R. Christensen and C. L. Cocke, Nucl. Phys. 89, 656 (1966).

[21]F. S. Dietrich, Nucl. Phys. 69, 49 (1965).

[22]C. L. Cocke, Ph.D. thesis, California Institute of Technology, Pasadena, California, 1967 (unpublished).

[23]S. S. Hanna, in *Isospin in Nuclear Physics*, edited by D. H. Wilkinson (North-Holland Publishing Company, Amsterdam, The Netherlands, 1969), p. 591.

[24]F. C. Barker, private communication.

PHYSICAL REVIEW C VOLUME 3, NUMBER 5 MAY 1971

Excitation of ^{20}Ne by 180° Electron Scattering

W. L. Bendel, L. W. Fagg, S. K. Numrich,* E. C. Jones, Jr., and H. F. Kaiser

Nuclear Physics Division, Naval Research Laboratory, Washington, D. C. 20390

(Received 10 December 1970)

States in ^{20}Ne have been studied by 180° inelastic electron scattering with incident energies of 39 and 56 MeV. A large scattering peak is found at each bombarding energy, showing excitation of a 1^+, $T=1$ state at 11.2 MeV, with transition radius $R = 2.53 \pm 0.15$ fm and radiation width $\Gamma_0 = 11 \pm 2$ eV. Other levels from 11 to 19 MeV are also excited.

I. INTRODUCTION

Electron scattering at 180° has proven particularly useful in exciting 1^+, $T=1$ states in even-even $T=0$ nuclei. As electric transitions are inhibited at 180°, magnetic transitions generally dominate, particularly magnetic dipole ($M1$) transitions. Inhibition of $\Delta T = 0$, $M1$ transitions[1] in these nuclei further increases the selectivity of observable peaks in 180° scattering data. The states most abundantly excited are thus 1^+, $T=1$ states, the analogs of low-lying states in isobaric nuclei. In addition, Kurath[2] has shown that the transition strength is concentrated in the lowest few such levels. Previous work[3,4] at 180° with ^{24}Mg and ^{28}Si has shown agreement with these predictions.

Preliminary results[5] on ^{20}Ne exhibited striking concentration of the strength into one level at 11.2 MeV. In this paper, we report data on 39- and 56-MeV electron scattering from ^{20}Ne up to an excitation energy of 20 MeV. These data are employed

to obtain transition radii and radiation widths. The results are used to identify analog states, as well as to give information on the structure of this nucleus through the use of Kurath's sum rule.[2]

II. THEORETICAL EQUATIONS

The data are analyzed using the model-independent plane-wave Born-approximation (PWBA) expressions given by Rosen, Raphael, and Überall.[6] The correction to the distorted-wave Born-approximation (DWBA) is obtained by use of the ratios of DWBA cross sections to PWBA values for $M1$ and $M2$ transitions which are given by Chertok, Johnson, and Sarkar.[7]

The reduced transition probability B for given magnetic multipolarity ML is related to the momentum transfer q by the equation [Ref. 6, Eq. (13a)]

$$G(q,L,R)\equiv\left[\frac{B(ML,q)}{B(ML,0)}\right]^{1/2}$$

$$=1-\frac{L+3}{L+1}\,\frac{(qR)^2}{2(2L+3)}+\frac{L+5}{L+1}\,\frac{(qR^*)^4}{8(2L+3)(2L+5)}-\cdots. \tag{1}$$

The parameters R and R^* are transition radii defined in Ref. 6. The radius R is approximately equal to the nuclear-matter radius and has averaged slightly less than $1.0A^{1/3}$ fm for $M1$ transitions in our work on masses 24–28. As the fourth-order term is too small for experimental determination here, we set $R^*=R$. Although R is a parameter useful for multipole determination, its model-independent physical significance is open to question.[8]

After DWBA corrections are made to the experimental cross sections for a given transition, they are used to obtain L, R, and the ground-state radiation width Γ_0. As in our previous work,[3,4,9] we employ the equations for magnetic transitions at 180°. In simple form, one obtains [Ref. 6, Eq. (5)]

$$\left(\frac{d\sigma}{d\Omega}\right)_{180^\circ}=C\left(\frac{q^LG}{k_1}\right)^2, \tag{2}$$

where k_1 is the initial electron momentum and

$$C=\frac{L+1}{L}\,\frac{\pi\alpha}{[(2L+1)!!]^2}B(ML,0).$$

The ratio of cross sections at two bombarding energies is independent of C and is used to determine the value of R for assumed values of L. Usually only one multipolarity L yields a reasonable value of R; this value of L is adopted together with the corresponding values of R and C.

The ground-state radiative width for the transition considered is given by [Ref. 6, Eq. (15a)]

$$\Gamma_0=\frac{8}{\alpha}C\omega^{2L+1}\frac{2J_0+1}{2J+1}G^2(\omega,L,R), \tag{3}$$

where ω is the excitation energy, and J_0 and J are the ground- and excited-state spins, respectively.

Similar equations for electric transitions may be obtained from Rosen, Raphael, and Überall.[6] We employ them in analysis of one case as an $E2$ transition, using the effective scattering angle (~178°). The DWBA corrections are obtained by interpolating in atomic number and momentum transfer (not incident energy) using the tables of Toepffer and Drechsel.[10] These tables are for the longitudinal part of the $E2$ interaction, not for the transverse part which dominates near 180°. However, they are judged to be more than sufficiently accurate for use with the small peaks, particularly as the DWBA correction factors for $M1$, $M2$, and $E2$ transitions are similar.

III. APPARATUS AND DATA TREATMENT

The source of the electrons utilized here is the U.S. Naval Research Laboratory 60-MeV linear accelerator, operated at 360 pulses per second. A beam of about 4 μA, with a full energy spread of 0.4% or 0.5%, was directed into the scattering chamber during the work on ^{20}Ne.

The target consisted of 5.08 cm of ^{20}Ne, cooled by liquid nitrogen and at 4.4 atm pressure, in a cylindrical chamber with end windows of 6-μm Havar foils. Scattered electrons are magnetically analyzed and a 0.5% momentum bin is counted by each of three scintillation telescopes. The electron scattering apparatus has been described more fully in a previous article[9] and the refrigerated gas target system has been described elsewhere.[11]

Allowance was made for variations in neon density due to pressure changes and due to beam heating. In general, the data were treated as in our previous work.[3] However, the Schwinger correction employed here follows the comments of Maximon.[12]

The area under a peak is integrated to about 1 to 1.5% below the peak energy and corrections made for the low-energy tail. We have, in the past, separately calculated and applied the corrections due to Schwinger, bremsstrahlung, and ionization-energy-loss distributions. Actually, these three distributions should be folded, together with the instrumental effects. The corrections will lower the energy of the peak position, and the instrumental line-shape width will increase the tail correction. Accordingly, a careful folding of instrumental effects with Schwinger,

bremsstrahlung, and ionization-energy-loss distributions was made for the 56-MeV data at 11.2-MeV excitation. The relationship of these results to the results using the previous method of calculating corrections was plotted as a function of integration interval below the peak energy. Thus, the results of the folding were employed directly for the peak considered and indirectly for other cases.

The uncertainties given for the cross sections are based on counting statistics and base-line uncertainties only. As R is based on the *ratio* of cross sections, the uncertainties given for R are based on those given for cross sections. The values given for radiation widths are absolute values, and an additional uncertainty of about 15% (actually 0.15 in $\ln\Gamma_0$) is included to allow for the absolute cross-section calibration and other factors.

The excitation-energy scales were initially based on the elastic peaks. However, the fringe field of the spectrometer magnet has a small effect on the incoming electron beam and therefore on the position of the beam as it passes through the gas chamber. As this effect is greatest for data taken at or near the elastic peak and is less important elsewhere, it is desirable to avoid calibration at the elastic peak. (The problem does not arise with solid targets, as the target may be easily replaced with a scintillator to check beam location, using a television system.) In addition, the neon elastic peak is not resolved from the elastic peak of the foils. While the foil peak can be observed with the chamber empty, it will be altered by the presence of gas and the correction for the foil peak is therefore not a simple subtraction. For these reasons, the excitation-energy scale is based on the 11.2-MeV peak, as described below.

IV. RESULTS

Data were obtained with ^{20}Ne and background data were obtained with the empty gas chamber. In addition, instrumental effects were studied by obtaining some data with the copper liner (see Fig. 2 of Ref. 11) removed from the gas chamber. As the amount of ^{20}Ne available was insufficient for use with the larger volume, natural neon was used in this case.

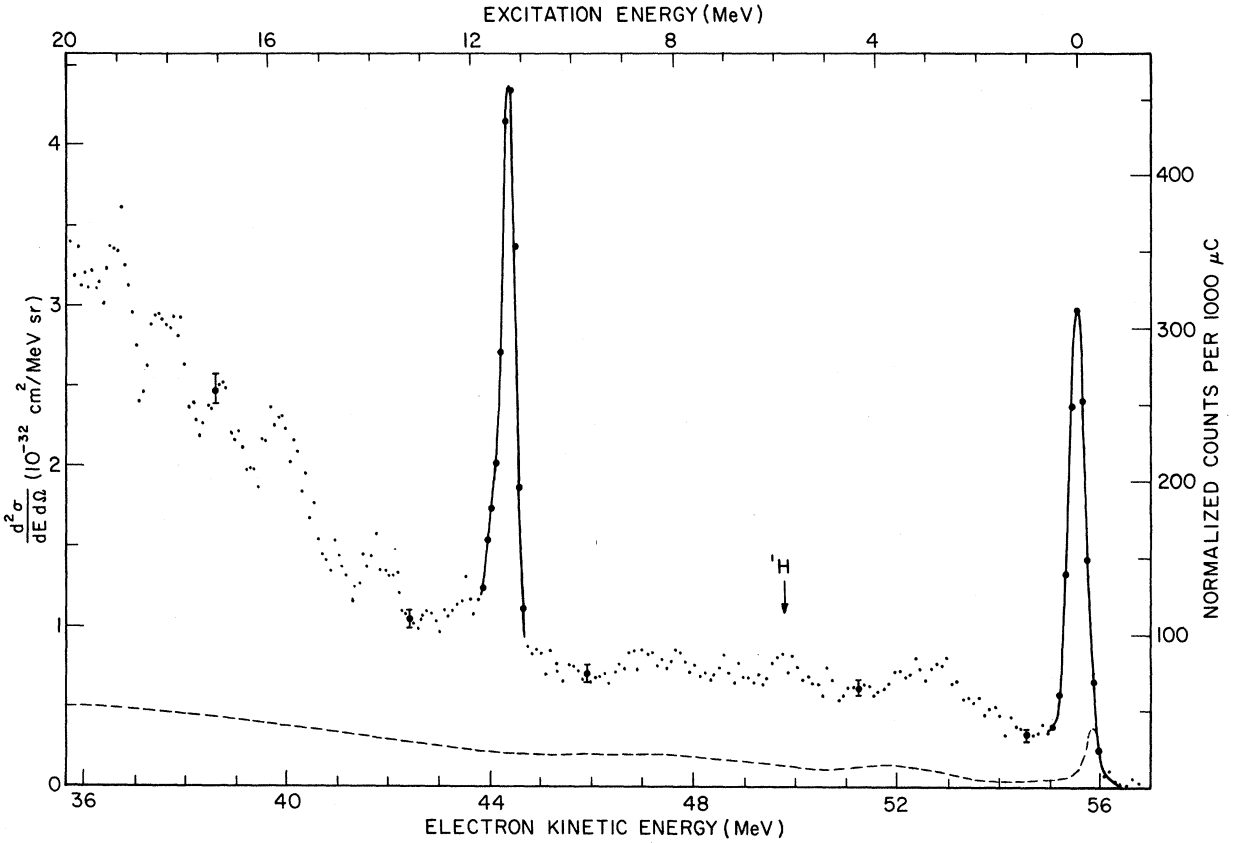

FIG. 1. Spectrum obtained by 180° scattering of 56-MeV electrons from ^{20}Ne. The dashed line shows the spectrum obtained with an evacuated chamber, in terms of counts per 1000 μC only.

The results of bombardment with 56-MeV electrons are shown in Fig. 1, from the elastic peak to an excitation of 20 MeV. The corresponding results with 39-MeV electrons are shown in Fig. 2. The energy scales at the top of the figures show calculated excitation, allowing for the recoil of ^{20}Ne. The counting rates are the values obtained after subtracting the counting rate with the spectrometer set for energies greater than the incident energy and then normalized to the bin width and solid angle corresponding to a kinetic energy of 35.22 MeV. The cross-section scales are obtained using the atoms/cm^2 of ^{20}Ne only. In each set of data, the elastic peak and the peak near 11-MeV excitation dominate the spectrum. The spectra obtained with an empty gas chamber are shown as dashed lines on the figures. These background data show an elastic peak due to the two 6-μm Havar foils, but no other peak.

The presence of gas produces counts due to the gas and also alters the "background" in two significant respects. As mentioned above, electrons scattered at ~180° in the second Havar foil are degraded in energy by passing through the gas, and the foil elastic peak will be split into two peaks. In addition, rather small-angle scattering in the gas will deflect electrons into the 1.11-cm-diam inner wall of the gas chamber, producing counts by double scattering. It is seen that a subtraction of vacuum data from ^{20}Ne data does not yield the true net ^{20}Ne spectrum. However, as the background data show no inelastic peaks, the ^{20}Ne inelastic peaks may be evaluated from the total spectra.

The elastic peak of hydrogen is indicated in each spectrum, at an apparent excitation energy due to the much larger recoil energy of ^{1}H. Although $\geq$99.9% of the neon was ^{20}Ne, there was a 0.3% hydrogen contaminant. The intensities of the observed peaks are in qualitative agreement with those expected from the work of Jones *et al.*[13] Data with natural neon at 56 MeV did not show a "6-MeV" peak, indicating that the sample was relatively free of hydrogen.

At excitations above 10 MeV, $T=1$ levels become available in ^{20}Ne and significant resonances are expected. In addition to the large peak, a number of smaller peaks are barely evident at about 12.0, 12.9, 13.9, 15.8, 16.9, 18.0, and 19.0 MeV. The data with natural neon confirm the

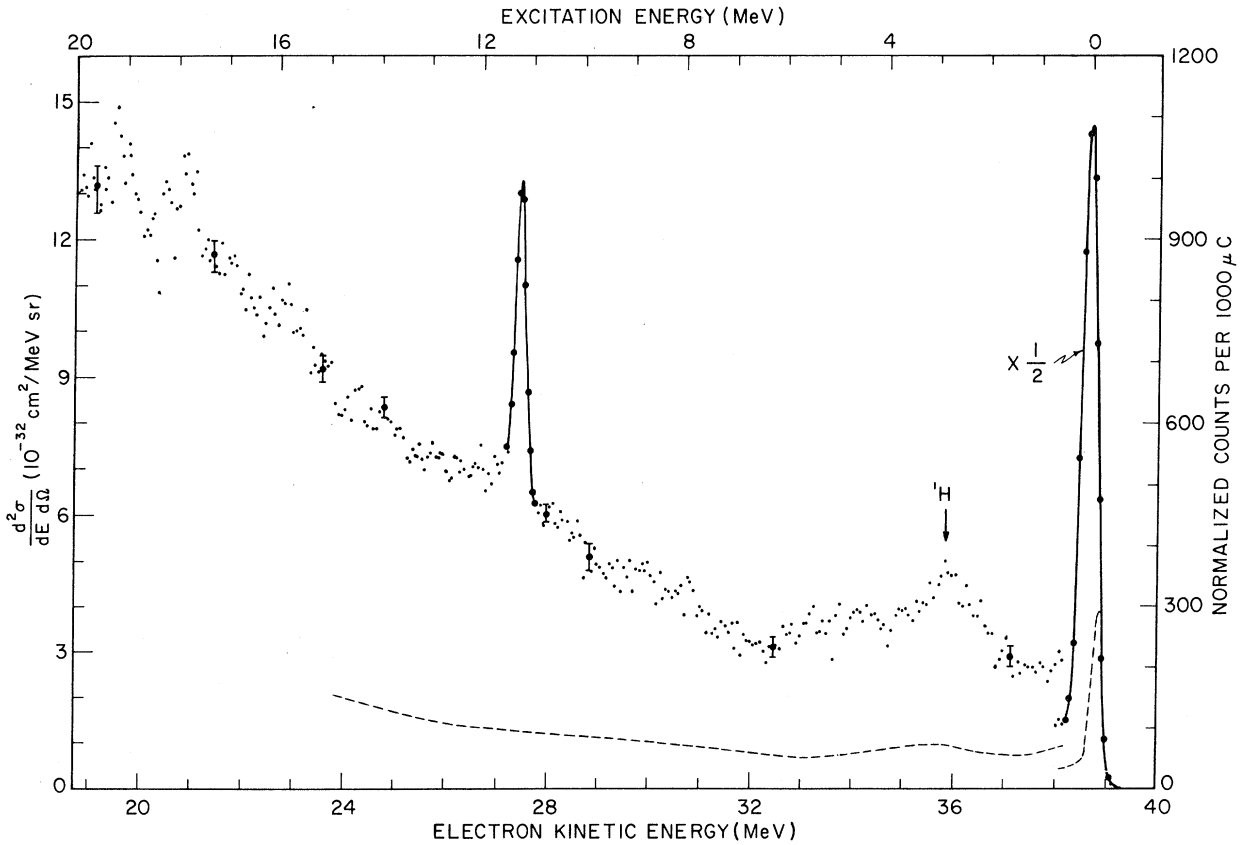

FIG. 2. Spectrum obtained by 180° scattering of 39-MeV electrons from ^{20}Ne. The dashed line shows the spectrum obtained with an evacuated chamber, in terms of counts per 1000 μC only.

TABLE I. Values of differential cross sections, spin and parity, transition radius, and radiation width for levels excited in ^{20}Ne, with DWBA corrections.

Level energy (MeV)	$(d\sigma/d\Omega)_{56}$ (10^{-34} cm^2/sr)	$(d\sigma/d\Omega)_{39}$ (10^{-34} cm^2/sr)	J^π	R (fm)	Γ_0 (eV)
11.235[a]	145 ± 5	219 ± 10	1^+	2.53 ± 0.15	$11.2^{+2.2}_{-1.8}$
11.58 ± 0.03	16 ± 4	13 ± 4	1^+	<1.8[b]	0.65 ± 0.18[b]
			2^+	<2.7[b]	0.40 ± 0.13[b]
			2^-	$4.1^{+1.0}_{-0.6}$	0.016 ± 0.009

[a] See Refs. 14 and 15.

[b] The value calculated for R^2 is negative, with a positive upper limit. Therefore, the value of Γ_0 is calculated assuming that R is between zero and the maximum value consistent with the data.

existence of most of these peaks. The electron scattering data do not show peaks at an excitation of 13.17 or 13.48 MeV, where 1^+, $T=1$ levels have been reported.[14]

Our peak at 11.2-MeV excitation has been identified[5] with the level found by Lawergren, Ferguson, and Morrison[15] and by Ritter, Parson, and Bernard.[14] However, with additional data, it became evident that the peak at each bombarding energy has a shoulder on the high-excitation side. An analysis of line shapes indicates that there is a main component, at an excitation energy of 11.22 ± 0.05 MeV on the initial energy scale, and a smaller component at about 0.345-MeV greater excitation. Basing our final energy scale on the identification of the main component with the level at 11.235 MeV,[14,15] the minor component is at 11.58 ± 0.03 MeV.

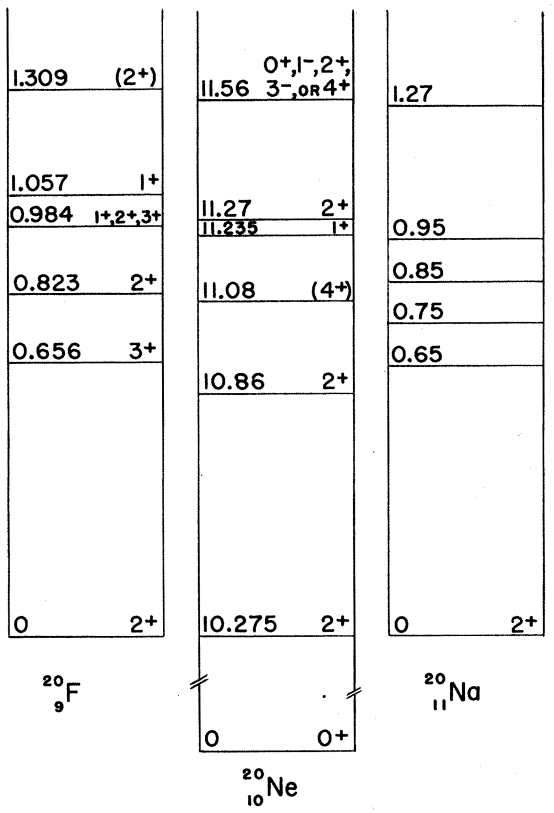

FIG. 3. Energy-level diagram of low-lying analog states in nuclei of mass 20. The energy scale is adjusted so that the lowest analog states are aligned.

V. DISCUSSION

The results show a remarkable concentration of inelastic scattering strength into one level. One expects magnetic dipole transitions to dominate in 180° electron scattering, and the ratio of the cross sections at the two bombarding energies does indeed fit this assignment, with $R = 2.53$ fm as given in Table I. As $M1$ transitions from the 0^+, $T=0$ ground state of ^{20}Ne to other $T=0$ states are inhibited,[1] the state at 11.235 MeV must be a 1^+, $T=1$ state and therefore the analog of a 1^+ state in ^{20}F.

When the results for the state at 11.58 MeV are analyzed assuming a magnetic transition, an assignment of $M2$ is indicated. However, analog-state considerations suggest an $E2$ assignment. As electric multipoles are sometimes seen weakly at 180°, we present the results of an $E2$ calculation in the table.

It is useful at this point to compare our results with other information on the lowest $T=1$ states of ^{20}Ne and their analogs. Figure 3 shows the lowest-energy $T=1$ states[14-18] of ^{20}Ne together with states[19,20] of ^{20}F and ^{20}Na in the corresponding energy range. It is seen that there is a marked similarity in these three nuclei. The 1^+ level in ^{20}Ne at 11.235 MeV, which dominates our spectra, appears to be the analog of the level at 1.057 MeV in ^{20}F. The highest ^{20}Ne level shown, which we observe at 11.58 MeV, is probably the analog of the 2^+ level at 1.309 MeV in ^{20}F. This ^{20}Ne level would be reached by an $E2$ transition here, a conclusion marginally consistent with the cross sections taken from the shoulders of the 11.2-MeV peaks at the two bombarding energies.

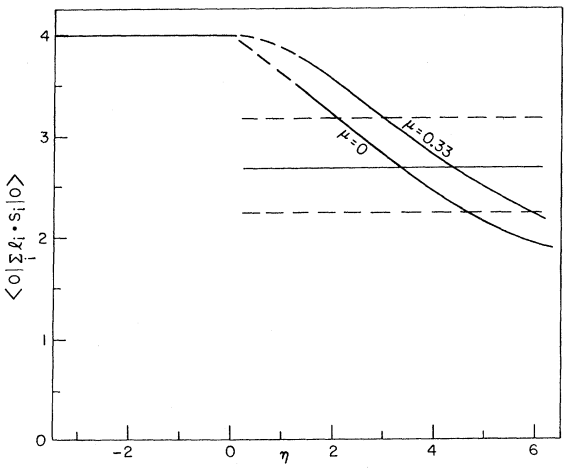

FIG. 4. The curves show the ground-state ls-coupling matrix element of ^{20}Ne as a function of deformation η according to the Nilsson model, for two values of μ. The value obtained from the 11.235-MeV level only, using $a = -2.03$ MeV, is shown by the horizontal line within the error limits indicated by the dashed lines.

None of the other peaks is large enough for a good quantitative analysis. Considerable transition strength is seen between 12- and 19-MeV excitation, but the multipolarity cannot be determined.

It is interesting to compare the distribution of magnetic dipole electron scattering in the $T=0$ even-even nuclei in the $2s$-$1d$ shell. In ^{20}Ne, we find a striking concentration of $M1$ strength into the lowest 1^+, $T=1$ level, and we see no peaks below 10.3 MeV, where only $T=0$ states can exist. In the case of ^{24}Mg, the strength is concentrated in the two lowest levels,[3] the second lowest being strongest. The dominant peak[4] in ^{28}Si represents the third-lowest 1^+, $T=1$ state. These three cases are in agreement with Kurath's prediction[2] that the $M1$ strength is concentrated in a few of the lowest-energy $T=1$ levels. Unlike these nuclei, the results[21] with ^{32}S show no large scattering peak.

The electron scattering results may be used with Kurath's work[2] to yield information on nuclear structure and deformation. Kurath relates the energy-weighted sum of the $M1$ transition strengths to the ground-state expectation value of the sum of the nucleon spin-orbit couplings, the other contributions being considered small for $I=0=T$ even-even nuclei. In terms of the quantities used here, the relationship is

$$\frac{0.614\ \text{MeV}}{-a}\sum_j \frac{\Gamma_{0j}}{\text{eV}}\left(\frac{10\ \text{MeV}}{\omega_{0j}}\right)^2 \cong \langle 0|\sum_i \vec{l}_i\cdot\vec{s}_i|0\rangle\ , \tag{4}$$

where Γ_{0j} is the radiative width of the $M1$ transition from the excited state of energy ω_{0j} to the ground state. We shall take the coupling parameter in the $1d$ shell to be $a=-2.03$ MeV, based on the 5.08-MeV state[19] and the ground state of ^{17}O.

In view of the dominance of the 11.2-MeV peak, one might initially evaluate the left side of this equation using only that level, obtaining a value of 2.67, with limits of 2.24 and 3.19, assuming the equation and the value of a to be exact. However, significant contributions to the sum can be made by levels at high excitation which do not show up as prominently in the spectra. The upper limit of the sum in Eq. (4) cannot therefore be evaluated solely on the basis of this one level.

We have calculated the right side of Eq. (4) versus deformation η, using Nilsson wave functions[22] for two values[23] of the parameter μ. One obtains 4.0 for all oblate deformations (orbit 5) and decreasing values with increasing prolate deformation (orbit 6). The results are compared with our one-level value in Fig. 4. Our single-level value places a lower limit on the sum and therefore places restrictions on the values of η, μ, and a which are acceptable in the Nilsson model.

Finally, it should be pointed out that the strong concentration of $M1$ strength into one level in ^{20}Ne is theoretically explained by Akiyama, Arima, and Sebe[24] in terms of a shell model based on $SU(3)$ symmetry. They note that the dominant part of the $M1$ operator is given by $\Sigma_i \tau_{3i}\sigma_i$, which cannot change the spatial symmetry. In particular, this operator cannot excite the main component of the ground-state wave function, $[4](80)^{11}S_{J=0}$, to a $T=1$, 1^+ state. It is then only by admixture of other states through spin-orbit coupling that an $M1$ transition can be effected by the above operator. Among the possible admixed states, the $[31](61)^{13}P_{J=0}$ is strongly dominant. Of the $T=1$, 1^+ states available for transitions from the latter state, only the $[31](61)^{33}P_{J=1}$ has nonvanishing strength.

VI. ACKNOWLEDGMENTS

We are indebted to Ralph Tobin and the linac staff for maintaining and operating the accelerator, and for assistance in many other tasks. Consultations with Professor H. Überall have proven invaluable, particularly in reference to the use of the Nilsson model. We thank Professor B. Chertok for his DWBA calculations. The continued advice and encouragement of Dr. T. F. Godlove is greatly appreciated.

*Now with Acoustics Division, Naval Research Laboratory, Washington, D. C.
[1]G. Morpurgo, Phys. Rev. 110, 721 (1958).
[2]D. Kurath, Phys. Rev. 130, 1525 (1963).
[3]L. W. Fagg, W. L. Bendel, R. A. Tobin, and H. F. Kaiser, Phys. Rev. 171, 1250 (1968).
[4]L. W. Fagg, W. L. Bendel, E. C. Jones, Jr., and S. Numrich, Phys. Rev. 187, 1378 (1969).
[5]W. L. Bendel, L. W. Fagg, E. C. Jones, Jr., H. F. Kaiser, and S. Numrich, Bull. Am. Phys. Soc. 13, 1373 (1968).
[6]M. Rosen, R. Raphael, and H. Überall, Phys. Rev. 163, 927 (1967).
[7]B. T. Chertok, W. T. K. Johnson, and D. Sarkar, *"Table of Coulomb Distortation Corrections to Inelastic Electron Scattering Cross Sections for Magnetic-Dipole & -Quadrupole Transitions"* (The American University, Department of Physics, Washington, D. C., 1970).
[8]D. Drechsel, Nucl. Phys. A113, 665 (1968).
[9]W. L. Bendel, L. W. Fagg, R. A. Tobin, and H. F. Kaiser, Phys. Rev. 173, 1103 (1968).
[10]C. Toepffer and D. Drechsel, Z. Physik 210, 423 (1968).
[11]L. W. Fagg, E. C. Jones, Jr., and W. L. Bendel, Nucl. Instr. Methods 77, 136 (1970).
[12]L. C. Maximon, Rev. Mod. Phys. 41, 193 (1969). We employ the equation for inelastic scattering at the bottom of p. 199, but in the part-exponential form of the equation on p. 201.
[13]E. C. Jones, Jr., *et al.*, to be published.
[14]R. C. Ritter, J. T. Parson, and D. L. Bernard, Phys. Letters 28B, 588 (1969).
[15]B. T. Lawergren, A. T. G. Ferguson, and G. C. Morrison, Nucl. Phys. A108, 325 (1968).
[16]J. D. Pearson and R. H. Spear, Nucl. Phys. 54, 434 (1964).
[17]R. M. Polichar, J. E. Steigerwalt, J. W. Sunier, and J. R. Richardson, Phys. Rev. 163, 1084 (1967).
[18]J. W. Sunier, A. J. Armini, R. M. Polichar, and J. R. Richardson, Phys. Rev. 163, 1091 (1967).
[19]C. M. Lederer, J. M. Hollander, and I. Perlman, *Table of Isotopes* (John Wiley & Sons, Inc., New York, 1967), 6th ed.
[20]P. A. Quin and S. E. Vigdor, Bull. Am. Phys. Soc. 15, 1686 (1970); P. A. Quin, G. A. Bissinger, and P. R. Chagnon, Nucl. Phys. A115, 495 (1970).
[21]L. W. Fagg, W. L. Bendel, L. Cohen, E. C. Jones, Jr., and H. Überall, Bull. Am. Phys. Soc. 15, 1665 (1970).
[22]S. G. Nilsson, Kgl. Danske Videnskab. Selskab, Mat.-Fys. Medd. 29, No. 16 (1955).
[23]G. R. Bishop, Nucl. Phys. 14, 376 (1959).
[24]Y. Akiyama, A. Arima, and T. Sebe, Nucl. Phys. A138, 273 (1969).

PHYSICAL REVIEW C VOLUME 3, NUMBER 5 MAY 1971

Quasielastic Electron Scattering from ^{3}He and ^{3}H†

D. R. Lehman*
Center for Radiation Research, National Bureau of Standards, Washington, D. C. 20234
(Received 9 December 1970)

Quasielastic electron scattering from ^{3}He and ^{3}H is investigated with a model in which the two-nucleon interaction is described by a separable potential. Cross sections are given in the impulse approximation for the ejected proton and scattered electron detected in coincidence, and for detection of only the scattered electron. Both two- and three-body breakup of ^{3}He and ^{3}H are considered, with final-state interactions between the spectator nucleons included in three-body breakup. Good agreement is obtained with all the electrodisintegration data, except the ^{3}He coincidence data, for wave functions derived from separable potentials which reproduce the s-wave two-nucleon phase shifts at low and medium energies. Rescattering corrections between the spectator particles are found to be important in calculating three-body disintegration. The need for more refined and reliable coincidence data is reaffirmed.

I. INTRODUCTION

Electron scattering is a powerful tool to probe the structure of the trinucleons, ^{3}He and ^{3}H, and to obtain information about nucleon-nucleon interactions. The electric charge and magnetic form factors of ^{3}He and ^{3}H, which provide information about the three-nucleon ground state, can be measured by elastic electron scattering. Electrons scattered inelastically from the trinucleons also are sensitive to the ground-state wave function, but such experiments also involve the three-nucleon continuum states. A great amount of work has been done both experimentally and theoretically on elastic electron scattering,[1,2] but the work on inelastic electron scattering from ^{3}He and ^{3}H has been more limited.

^{3}He and ^{3}H inelastic electron scattering experiments have involved both low and high nuclear excitation energies, but no pion production. The most recent experiments have been concerned with the threshold region.[3] Frosch *et al.* have searched for excited states of ^{3}He by measuring inelastic spectra up to 17-MeV excitation energy.